FINITE ELASTICITY

by
Stephen V. Harren
http://www.harren.us

Contents

1. Strain Measures

The deformation gradient F is defined by

$$\mathrm{d}x_i = F_{ij}\mathrm{d}X_j \ , \tag{1.1}$$

where $\mathrm{d}X_i$ is a differential vector of material particles in the undeformed configuration, which same material vector in the deformed configuration is $\mathrm{d}x_i$. The only restriction on F is $\det F > 0$. By the Polar Decomposition Theorem, F can be decomposed as

$$F = VR \ , \tag{1.2}$$

where V is the (symmetric) left stretch tensor (whose eigenvalues are positive), and R is the rotation tensor.

To calculate V, consider

$$B = FF^T = VRR^TV = VIV = VV \ , \qquad i.e., \quad V = \sqrt{B} \, . \tag{1.3}$$

Typically, the square root in eqn. (1.3) is calculated by solving a three-dimensional eigenproblem. Numerically, though, using Babylonian (or Hero's) iteration is more reliable. The scalar form of the iteration is

$$x^{\mathrm{imp}} = \frac{1}{2}\left(x + \frac{S}{x}\right) \ , \tag{1.4}$$

where x is a guess for $\sqrt{S}$ and x^{imp} is an improved guess. Equation (1.4) calculates $\sqrt{99}$ to 10 digits of accuracy with 8 iterations. The tensorial form of eqn. (1.4) is

$$V_{kl}^{\mathrm{imp}} = \frac{1}{2}V_{kl} + \frac{1}{4}\left(B_{kj}V_{jl}^{-1} + B_{lj}V_{jk}^{-1} \right) . \tag{1.5}$$

When implementing eqn. (1.2) in a finite element program, the gradients $\partial V_{ij}/\partial F_{pq}$ are required. Consequently, by differentiating $B = VV$, one obtains

$$\frac{\partial B_{ij}}{\partial V_{pq}} = I_{ikpq}V_{kj} + V_{ik}I_{kjpq} \quad \text{with} \quad I_{ijkl} = \frac{1}{2}\left(\delta_{ik}\delta_{jl} + \delta_{jk}\delta_{il} \right) \ , \tag{1.6}$$

where I_{ijkl} is the fourth order fully symmetric identity tensor, and δ_{ij} are the components of the three-dimensional identity matrix (or Kronecker delta). Notwithstanding, $\partial V_{ij}/\partial B_{pq}$ is the inverse of $\partial B_{ij}/\partial V_{pq}$, which inverse may be calculated from eqns. (1.6) by inverting a 6×6 matrix. Next, differentiation of $B = FF^T$ gives

$$\frac{\partial B_{ij}}{\partial F_{pq}} = \delta_{ip}F_{jq} + F_{iq}\delta_{jp} \, . \tag{1.7}$$

Finally, by the chain rule,

$$\frac{\partial V_{ij}}{\partial F_{pq}} = \frac{\partial V_{ij}}{\partial B_{kl}}\frac{\partial B_{kl}}{\partial F_{pq}} \ . \tag{1.8}$$

The strain measure most appropriate for finite elasticity is the true (or logarithmic) strain ε, which is defined via

$$\varepsilon = \ln V . \tag{1.9}$$

Again, typically, the logarithm in eqn. (1.9) is calculated by diagonalizing V, and by taking the logarithms

of the eigenvalues of V. Numerically, a Taylor series is more reliable. In the scalar case

$$\ln x = \sum_{i=0}^{N} \frac{2}{2i+1}\left(\frac{x-1}{x+1}\right)^{2i+1} \qquad N \to \infty \ , \tag{1.10}$$

which series converges for all x. For example, the series (1.10) calculates ln 12 to 9 digits of accuracy with $N = 49$ (*i.e.,* 50 terms). Letting

$$A_{ij} = \frac{1}{2}\left(C_{ik}D_{kj} + C_{jk}D_{ki} \right) \ \text{ with } \quad C = V - I \quad \text{and} \quad D = (V+I)^{-1} \ , \tag{1.11}$$

the tensorial form of eqn. (1.10) is

$$\varepsilon = \ln V = \sum_{i=0}^{N} \frac{2}{2i+1} A^{2i+1} \ . \tag{1.12}$$

When one calculates the derivatives $\partial \varepsilon_{ij}/\partial V_{pq}$ of eqn. (1.12), untenably long expressions are obtained after only a few terms. Thus, in a finite element code, central difference is used. For example,

$$\frac{\partial \varepsilon_{ij}}{\partial V_{01}} = \frac{\varepsilon_{ij}^{+} - \varepsilon_{ij}^{-}}{\Delta} \ , \qquad \varepsilon_{ij}^{+} = \varepsilon_{ij}(V^{+}) \ , \qquad \varepsilon_{ij}^{-} = \varepsilon_{ij}(V^{-}) \ ,$$

$$V^{+} = V + \frac{1}{2}\begin{bmatrix} 0 & \Delta & 0 \\ \Delta & 0 & 0 \\ 0 & 0 & 0 \end{bmatrix} \ , \qquad V^{-} = V - \frac{1}{2}\begin{bmatrix} 0 & \Delta & 0 \\ \Delta & 0 & 0 \\ 0 & 0 & 0 \end{bmatrix} \ , \qquad etc. \tag{1.13}$$

In the numerical calculations of Sec. 6 below, $\Delta = 0.001$ is used.

As an example of the above calculational procedure, letting

$$F = \begin{bmatrix} 0.750 & 0.25 & 0.50 \\ -0.125 & 1.50 & -0.75 \\ -1.750 & 2.00 & 1.25 \end{bmatrix} \ , \tag{1.14}$$

eqn. (1.5) gives, using 10 iterations,

$$V = \begin{bmatrix} 0.933\,900 & -0.027\,895\,4 & -0.045\,306\,0 \\ -0.027\,895\,4 & 1.603\,16 & 0.507\,169 \\ -0.045\,306\,0 & 0.507\,169 & 2.892\,36 \end{bmatrix} \ , \tag{1.15}$$

and then eqn. (1.12) yields, using 50 terms,

$$\varepsilon = \begin{bmatrix} -0.069\,092\,3 & -0.018\,849\,2 & -0.024\,117\,6 \\ -0.018\,849\,2 & 0.437\,725 & 0.236\,368 \\ -0.024\,117\,6 & 0.236\,368 & 1.038\,92 \end{bmatrix} . \tag{1.16}$$

The results (1.15) and (1.16) have been verified by solving the corresponding eigenproblems by hand.

2. Uniaxial Response

Figure 1 below shows the uniaxial stress-strain curve for vulcanized rubber. The blue plotted points in the figure are the experimental data of Treloar (1940), see the "Herve Marand Rubber Elasticity Lecture 17" (`eng.uc.edu`). While the author is not quite sure of the exact meaning of σ and ε in the figure, herein they will be interpreted as being true stress and true (or logarithmic) strain. The red curve in the figure is a piecewise cubic fit to the data, which fit is constructed as follows. The ε–axis is broken into

n subintervals, the ith one of which is depicted below in Fig. 2. The normalized coordinate $\xi \in (-1,1)$ in the figure is

$$\xi = \frac{2\varepsilon - \varepsilon^{i+1} - \varepsilon^{i}}{L} \ , \qquad L = \varepsilon^{i+1} - \varepsilon^{i} \ . \tag{2.1}$$

Now, in each subinterval $i \in (0, n-2)$, the uniaxial stress is written as

$$\sigma = a^0\sigma^i + a^1 m^i + a^2\sigma^{i+1} + a^3 m^{i+1} \ , \tag{2.2}$$

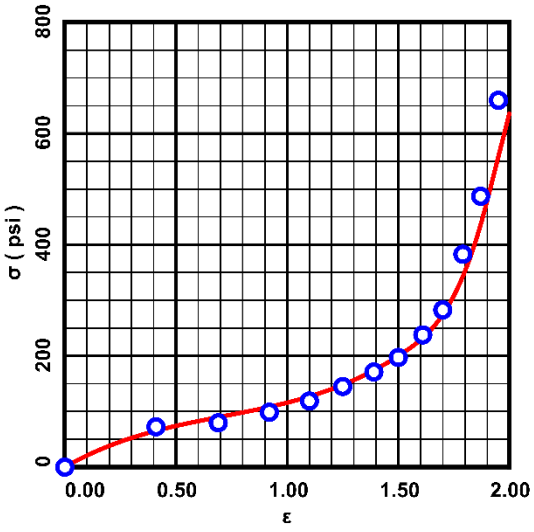

Figure 1. Stress-strain data for vulcanized rubber as explained in the text.

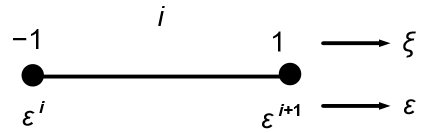

Figure 2. Normalized subinterval.

where, *e.g.*, m^i is the slope of the stress-strain curve at point i in Fig. 2, and

$$\begin{aligned} a^0 &= \frac{1}{4}(2 - 3\xi + \xi^3) \ , \\ a^1 &= \frac{L}{8}(1 - \xi - \xi^2 + \xi^3) \ , \\ a^2 &= \frac{1}{4}(2 + 3\xi - \xi^3) \ , \\ a^3 &= \frac{L}{8}(-1 - \xi + \xi^2 + \xi^3) \ . \end{aligned} \tag{2.3}$$

The derivative of eqn. (2.2) is

$$\frac{\mathrm{d}\sigma}{\mathrm{d}\varepsilon} = a^0_{,\varepsilon}\sigma^i + a^1_{,\varepsilon} m^i + a^2_{,\varepsilon}\sigma^{i+1} + a^3_{,\varepsilon} m^{i+1} \ , \tag{2.4}$$

with

$$\begin{aligned} a^0_{,\varepsilon} &= \frac{3}{2L}(-1 + \xi^2) \ , \qquad a^1_{,\varepsilon} = \frac{1}{4}(-1 - 2\xi + 3\xi^2) \ , \\ a^2_{,\varepsilon} &= \frac{3}{2L}(1 - \xi^2) \ , \qquad a^3_{,\varepsilon} = \frac{1}{4}(-1 + 2\xi + 3\xi^2) \ . \end{aligned} \tag{2.5}$$

Finally, for the last subinterval $i = n - 1$ (*i.e.*, for $\varepsilon > \varepsilon^{n-1}$), the response is taken as linear, *viz.*,

$$\sigma = m^{n-1}(\varepsilon - \varepsilon^{n-1}) + \sigma^{n-1} \ , \qquad \frac{\mathrm{d}\sigma}{\mathrm{d}\varepsilon} = m^{n-1} \ . \tag{2.6}$$

Thus, the red curve in Fig. 1 above is constructed with $n = 3$ and the constants

$$\begin{aligned} &\varepsilon^0 = 0 \ , && \varepsilon^1 = 1.5 \ , && \varepsilon^2 = 1.9 \\ &\sigma^0 = 0 \text{ psi} \ , && \sigma^1 = 200 \text{ psi} \ , && \sigma^2 = 460 \text{ psi} \ , \\ &m^0 = 230 \text{ psi} \ , && m^1 = 260 \text{ psi} \ , && m^2 = 1570 \text{ psi} \ . \end{aligned} \tag{2.7}$$

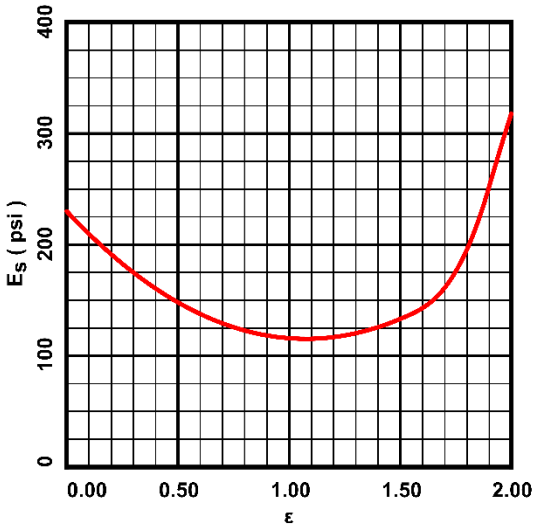

Figure 3. The secant modulus E_s.

Additionally, the secant modulus is

$$E_s = \frac{\sigma}{\varepsilon}\,, \tag{2.8}$$

which is graphed at right in Fig. 3. Finally, differentiation of eqn. (2.8) yields

$$\frac{\mathrm{d}E_s}{\mathrm{d}\varepsilon} = \frac{1}{\varepsilon}\left(\frac{\mathrm{d}\sigma}{\mathrm{d}\varepsilon} - E_s\right)\,. \tag{2.9}$$

3. Multiaxial Response and Stress Measures

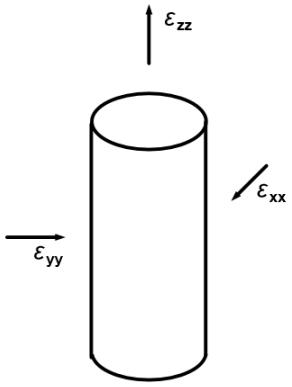

Figure 4. A specimen subjected to a uniaxial stress σ_{zz}.

Figure 4 at left depicts a tension specimen subjected to a uniaxial loading. The logarithmic strain component ε_{zz} is positive, and $\varepsilon_{xx} = \varepsilon_{yy} = -\nu\varepsilon_{zz}$, where ν is Poisson's ratio. For the situation in Fig. 4, $\varepsilon_{ij}\varepsilon_{ij} = (1+2\nu^2)\varepsilon_{zz}^2$, which gives the definition of the effective strain $\bar{\varepsilon}$, *viz.,*

$$\bar{\varepsilon} = \sqrt{\frac{\varepsilon_{ij}\varepsilon_{ij}}{1+2\nu^2}}\,. \tag{3.1}$$

Note that for uniaxial tension $\bar{\varepsilon}$ corresponds to the major uniaxial strain.

Now, for three-dimensional linear elasticity, Hooke's Law is

$$\sigma_{ij} = C^0_{ijkl}\varepsilon_{kl}\ , \qquad C^0_{ijkl} = \frac{E}{(1+\nu)(1-2\nu)}\left[\,(1-2\nu)I_{ijkl} + \nu\delta_{ij}\delta_{kl}\,\right], \tag{3.2}$$

where E is Young's modulus. A reasonable extension of eqn. (3.2) to finite elasticity is to replace Young's modulus with the secant modulus, and to take Poisson's ratio to be constant. Thus,

$$\sigma_{ij} = C_{ijkl}\varepsilon_{kl}\ , \qquad C_{ijkl} = \frac{E_s}{(1+\nu)(1-2\nu)}\left[\,(1-2\nu)I_{ijkl} + \nu\delta_{ij}\delta_{kl}\,\right]. \tag{3.3}$$

In eqn. (3.3), E_s is given by eqn. (2.8) with $\varepsilon \to \bar{\varepsilon}$, and $\sigma = \sigma(\varepsilon)$ in Sec. 2 is now $\sigma = \sigma(\bar{\varepsilon})$. Also, σ_{ij} is interpreted here as being the components of the true stress (σ_{ij} is the force per unit deformed area acting on the face whose normal is in the i–direction in the deformed configuration, with the force acting in the j–direction of the deformed configuration), and ε_{ij} are the components of the true strain.

The gradients of eqn. (3.3), *i.e.,* $\partial\sigma_{ij}/\partial\varepsilon_{kl}$, are required for use in a finite element program. Consequently, we have the derivatives

$$\frac{\partial\bar{\varepsilon}}{\partial\varepsilon_{pq}}=\frac{\varepsilon_{pq}}{(1+2\nu^2)\bar{\varepsilon}}\ ,\qquad \frac{\mathrm{d}E_s}{\mathrm{d}\bar{\varepsilon}}=\frac{1}{\bar{\varepsilon}}\left(\frac{\mathrm{d}\sigma}{\mathrm{d}\bar{\varepsilon}}-E_s\right)\ ,\qquad \frac{\partial C_{ijkl}}{\partial\bar{\varepsilon}}=\frac{1}{E_s}\frac{\mathrm{d}E_s}{\mathrm{d}\bar{\varepsilon}}C_{ijkl}\ ,$$
$$\frac{\partial C_{ijkl}}{\partial\varepsilon_{pq}}=\frac{\partial C_{ijkl}}{\partial\bar{\varepsilon}}\frac{\partial\bar{\varepsilon}}{\partial\varepsilon_{pq}}\ ,\qquad \frac{\partial C_{ijkl}}{\partial\varepsilon_{pq}}=\frac{1}{(1+2\nu^2)\sigma}\frac{\mathrm{d}E_s}{\mathrm{d}\bar{\varepsilon}}C_{ijkl}\varepsilon_{pq}\ . \tag{3.4}$$

Now, differentiating the first of eqns. (3.3) gives

$$\frac{\partial\sigma_{ij}}{\partial\varepsilon_{pq}}=\frac{\partial C_{ijkl}}{\partial\varepsilon_{pq}}\varepsilon_{kl}+C_{ijkl}\frac{\partial\varepsilon_{kl}}{\partial\varepsilon_{pq}} \tag{3.5}$$

so that, from the last of eqns. (3.4),

$$\frac{\partial\sigma_{ij}}{\partial\varepsilon_{pq}}=C_{ijkl}\left[I_{klpq}+\frac{1}{(1+2\nu^2)\sigma}\frac{\mathrm{d}E_s}{\mathrm{d}\bar{\varepsilon}}\varepsilon_{kl}\varepsilon_{pq}\right]\ . \tag{3.6}$$

We now turn attention to the nominal stress N_{ij}, given by

$$N_{kj}=(\det F)F^{-1}_{ki}\sigma_{ij}\ . \tag{3.7}$$

The component N_{ij} is the force per unit undeformed area acting on the face whose normal is in the i–direction in the undeformed configuration, with the force acting in the j–direction of the deformed configuration. Now, for square matrices in general,

$$\frac{\partial\det a}{\partial a_{ij}}=(\det a)a^{-T}_{ij}\ ,\qquad \frac{\partial a^{-1}_{lk}}{\partial a_{pq}}=-a^{-1}_{lp}a^{-1}_{qk} \tag{3.8}$$

so that the derivative of eqn. (3.7) is

$$\frac{\partial N_{kj}}{\partial F_{pq}}=F^{-1}_{qp}N_{kj}-F^{-1}_{kp}N_{qj}+(\det F)F^{-1}_{ki}\frac{\partial\sigma_{ij}}{\partial F_{pq}}\ , \tag{3.9}$$

where, by the chain rule,

$$\frac{\partial\sigma_{ij}}{\partial F_{pq}}=\frac{\partial\sigma_{ij}}{\partial\varepsilon_{kl}}\frac{\partial\varepsilon_{kl}}{\partial V_{mn}}\frac{\partial V_{mn}}{\partial F_{pq}}\ . \tag{3.10}$$

4. Equilibrium Equations

Equilibrium is

$$N_{ij,i}=0\ , \tag{4.1}$$

where the comma denotes differentiation with respect to the coordinates of the undeformed configuration. Now, let u^*_j be an arbitrary, once-differentiable vector field (the so-called virtual displacement). Then, multiplying eqn. (4.1) by u^*_j, *i.e.,* $u^*_jN_{ij,i}=0$, and then by the product rule of differentiation, $\left(u^*_jN_{ij}\right)_{,i}=$ $=u^*_{j,i}N_{ij}+u^*_jN_{ij,i}$, eqn. (4.1) becomes

$$u^*_{j,i}N_{ij}=\left(u^*_jN_{ij}\right)_{,i}\ . \tag{4.2}$$

Next, integrate eqn. (4.2) over the volume of the domain V, and use the Divergence Theorem to obtain

$$\int_V u^*_{j,i} N_{ij} \mathrm{d}V = \int_S u^*_j T_j dS \ , \tag{4.3}$$

which is the Principle of Virtual Work. In eqn. (4.3), S is the bounding surface of domain V, and $T_j = n_i N_{ij}$ is the nominal traction vector (**n** is the outward-pointing unit normal vector on S).

5. Brick Element and Finite Element Equations

Figure 5 below depicts the 8–noded isoparametric finite element in **ξ**–space, where $\xi_i \in (-1,1)$. In terms of the functions

$$f^0(s) = \frac{1}{2}(1-s) \ , \qquad f^1(s) = \frac{1}{2}(1+s) \ , \tag{5.1}$$

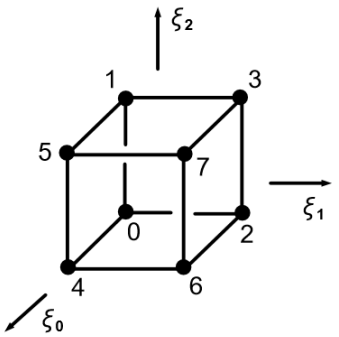

Figure 5. Brick element in **ξ**–space.

the eight shape functions S^I are given by the tensor product

$$\begin{aligned} S^0 &= f^0(\xi_0) f^0(\xi_1) f^0(\xi_2) \quad S^1 = f^0(\xi_0) f^0(\xi_1) f^1(\xi_2) \\ S^2 &= f^0(\xi_0) f^1(\xi_1) f^0(\xi_2) \quad S^3 = f^0(\xi_0) f^1(\xi_1) f^1(\xi_2) \\ S^4 &= f^1(\xi_0) f^0(\xi_1) f^0(\xi_2) \quad S^5 = f^1(\xi_0) f^0(\xi_1) f^1(\xi_2) \\ S^6 &= f^1(\xi_0) f^1(\xi_1) f^0(\xi_2) \quad S^7 = f^1(\xi_0) f^1(\xi_1) f^1(\xi_2) \end{aligned} \ . \tag{5.2}$$

The mapping to **x**–space (in the undeformed configuration) is given by

$$x_i = S^I x^I_i \ , \tag{5.3}$$

where x^I_i are the coordinates of the nodes. Now,

$$\mathrm{d}x_i = A_{i\alpha} \mathrm{d}\xi_\alpha \ , \qquad A_{i\alpha} = \frac{\partial x_i}{\partial \xi_\alpha} = S^I_{,\alpha} x^I_i \ , \qquad \frac{\partial \xi_\alpha}{\partial x_i} = A^{-1}_{\alpha i} \ , \tag{5.4}$$

so that volume integrals transform as

$$\int_{V^{\mathrm{x}}} (\ ) \mathrm{d}V^{\mathrm{x}} = \int_{V^{\xi}} (\ ) (\det A) \mathrm{d}V^{\xi} \ , \tag{5.5}$$

where $\mathrm{d}V^{\mathrm{x}}$ is a differential of volume in **x**–space and $\mathrm{d}V^{\xi}$ is a differential of volume in $\boldsymbol{\xi}-$space. Numerically, the volume integrations are evaluated with the 3–point Gauss-Legendre quadrature rule, which rule will integrate a fifth order polynomial exactly. Also consistent with eqns. (5.4), the (physical) gradients of the shape functions (in **x**–space) are, by the chain rule,

$$S^I_{,i} = S^I_{,\alpha} A^{-1}_{\alpha i} \ . \tag{5.6}$$

Turning attention now to the Principle of Virtual Work (4.3), interpolate the virtual displacement and its gradient through the element via

$$u^*_j = S^I u^{*I}_j \ , \qquad u^*_{j,i} = S^I_{,i} u^{*I}_j \ , \tag{5.7}$$

where u^{*I}_j are the nodal values of u^*_j. Substitution of eqns. (5.7) into eqn. (4.3) yields

$$u^{*I}_j \int_V S^I_{,i} N_{ij} \mathrm{d}V = u^{*I}_j \int_S S^I T_j dS \ , \tag{5.8}$$

or since u^{*I}_j is arbitrary,

$$\int_V S^I_{,i} N_{ij} \mathrm{d}V = \int_S S^I T_j dS \ , \tag{5.9}$$

Equations (5.9) constitute a nonlinear system, so it is solved with Newton-Raphson iteration. The residual is

$$r^I_j = \int_V S^I_{,i} N_{ij} \mathrm{d}V - \int_S S^I T_j dS = 0 \, . \tag{5.10}$$

Now, interpolate the displacement and its gradient through the element with

$$u_j = S^I u^I_j \ , \qquad u_{j,i} = S^I_{,i} u^I_j \ , \tag{5.11}$$

where u^I_j are the nodal values of the displacement. The components of the deformation gradient, and its derivative with respect to the nodal displacements, are then

$$F_{pq} = \delta_{pq} + u_{p,q} = \delta_{pq} + S^I_{,q} u^I_p \ , \qquad \frac{\partial F_{pq}}{\partial u^J_k} = S^J_{,q} \delta_{pk} \ . \tag{5.12}$$

Thus, from the second of eqns. (5.12),

$$\frac{\partial N_{ij}}{\partial u^J_k} = \frac{\partial N_{ij}}{\partial F_{pq}} \frac{\partial F_{pq}}{\partial u^J_k} = \frac{\partial N_{ij}}{\partial F_{kl}} S^J_{,l} \ . \tag{5.13}$$

The iteration equations are then

$$\frac{\partial r^I_j}{\partial u^J_k} \Delta u^J_k = J^{IJ}_{jk} \Delta u^J_k = -r^I_j \ , \qquad u^J_k \leftarrow u^J_k + \Delta u^J_k \ , \tag{5.14}$$

where the Jacobian is

$$J^{IJ}_{jk} = \int_V S^I_{,i} \frac{\partial N_{ij}}{\partial u^J_k} \mathrm{d}V = \int_V S^I_{,i} \frac{\partial N_{ij}}{\partial F_{kl}} S^J_{,l} \mathrm{d}V \, , \tag{5.15}$$

which was obtained by differentiating eqn. (5.10) and by using eqn. (5.13). In the numerical calculations which follow in Sec. 6, the iteration was deemed converged when all Δu^J_k satisfy

$$\left| \Delta u^J_k \right| \le 10^{-4} \max \left| u^J_k \right| \ . \tag{5.16}$$

For the stepping scheme described below in Sec. 6, convergence was generally achieved after about 10 to 12 iterations.

6. Numerical Example – Drawing of a Tension Specimen

The above constitutive behavior and finite element formulation is used to solve the problem of necking and drawdown of a uniaxial tension specimen, which specimen is shown below in Fig. 6. The specimen is a square prism with dimensions $2w \times 2w \times 2L$, where $L = 3$ in. Due to symmetry, only the first octant $x_i > 0$ is analyzed numerically. To initiate the necking, the width of the specimen is taken as

$$w = \frac{w_0}{2} \left[\, 2 - f - f \cos\left(\frac{\pi x_2}{L} \right) \right] \ , \tag{6.1}$$

with $w_0 = 0.25$ in and $f = 0.05$. In other words, $w(L) = w_0$ and $w(0) = 0.95 w_0$. The boundary conditions on the first octant are

$$u_0 = 0 \text{ and } T_1 = T_2 = 0 \text{ on } x_0 = 0\ , \quad u_1 = 0 \text{ and } T_0 = T_2 = 0 \text{ on } x_1 = 0\ ,$$
$$u_2 = 0 \text{ and } T_0 = T_1 = 0 \text{ on } x_2 = 0\ , \quad u_2 = U \text{ and } T_0 = T_1 = 0 \text{ on } x_2 = L\ , \qquad (6.2)$$
$$T_i = 0 \text{ on } x_0 = x_1 = w\ .$$

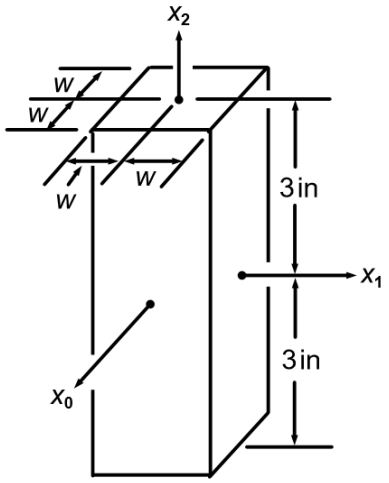

Figure 6. Uniaxial tension specimen.

Finally, $\nu = 0.45$ is used in the calculations.

The prescribed displacement on the top face of the specimen U was applied to the finite element mesh in the following fashion. The solution is started out with a linear elastic solution. The initial guess to the first displacement step is then the linear elastic solution scaled to fit the boundary conditions for the first displacement step. For subsequent displacement steps, the initial guess for the solution is the (nonlinear) solution for the nodal displacements of the pervious displacement step (again, scaled to fit the boundary conditions for the current displacement step). The table below shows the displacement steps that were applied to the finite element mesh for the analysis, where U is in inches.

step	0	1	2	3	4	5	6	7	8	9	10	11	12	13
U	1.0	1.5	2.0	2.1	2.2	2.3	2.4	2.5	2.6	2.7	2.8	2.9	3.0	3.1

14	15	16	17	18	19	20	21	22	23	24	25	26	27
3.2	3.3	3.4	3.5	3.6	3.7	3.8	3.9	4.0	4.1	4.2	4.3	4.4	4.5

Figure 7 below shows the nodes on the octant face $x_0 = 0$ for $U = 0$. The mesh used consists of a 5×5 array of nodes in the x_0x_1–plane, with 145 copies of these nodes stacked in the x_2–direction, resulting in 3625 nodes and 2304 elements.

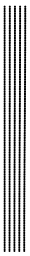

Figure 7. Plan view of specimen at $U = 0$ in.

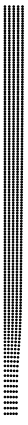

Figure 8. Plan view of specimen at $U = 2.0$ in.

Figures 8 through 10 show the deformed grid of nodes at various strain levels. Note that all the Figs. 7 through 10 possess the same scale. Notwithstanding, as Fig. 8 shows, at $U = 2.0$ in, the necking has commenced, and as seen from Figs. 9 and 10, drawdown of the specimen is occurring.

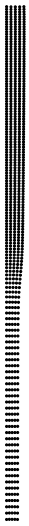

Figure 9. Plan view of specimen at $U = 3.3$ in.

Figure 10. Plan view of specimen at $U = 4.5$ in.

Figures 11 and 12 show, respectively, the true strain component ε_{22} and true stress component σ_{22} as functions of x_2 (*i.e.,* the axial coordinate in the undeformed configuration). The strain and stress values are from the centers of the column of elements which abut the x_2–axis. As the figures show, the transition zone between the drawn and undrawn portions of the specimen is highly evident.

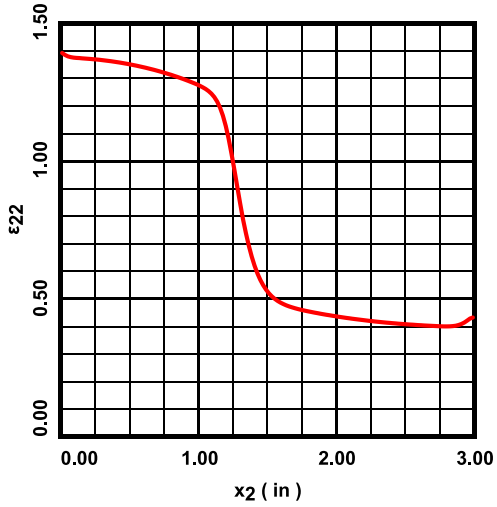

Figure 11. Strain component ε_{22} at $U = 4.5$ in.

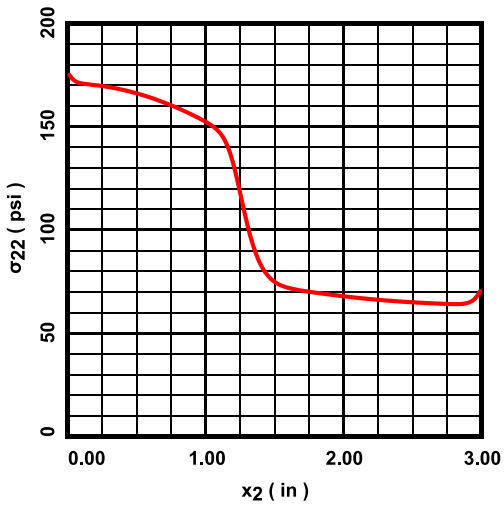

Figure 12. Stress component σ_{22} at $U = 4.5$ in.

7. Closing Remarks

While the calculations easily may be carried out to higher strain levels, the viability of the calculational procedure has been demonstrated. Before implementing the procedures described above in Sec. 1 concerning the calculation of the tensors V and ε, the author originally tried solving for them with three-dimensional eigenproblems, which approach proved to be cumbersome and unreliable. One notes that this difficulty will not occur in two-dimensional analyses, as the eigenproblems are easily solved for explicitly.